

Freezing of Ni–Al Bimetallic Nanoclusters in Computer Simulations

Yaroslav G. Chushak and Lawrence S. Bartell*

Department of Chemistry, University of Michigan, Ann Arbor, Michigan 48109

Received: December 3, 2002; In Final Form: February 21, 2003

Bimetallic particles have two features not observed in one-component systems: surface segregation and compositional ordering. Molecular dynamics simulations have been performed to study the freezing of Ni–Al nanoclusters at different compositions. It was found that for Al-rich and equiatomic compositions the surface segregation of Al atoms inhibits nucleation, causing supercooled clusters to solidify to an amorphous aggregate. In the case of Ni₃Al particles, where there are not enough Al atoms to complete the surface layer, clusters froze to multiply twinned structures with well-defined local translational order but, owing to the fast kinetics of solidification, with compositional disorder.

I. Introduction

Metal nanoparticles, comprised of hundreds or up to thousands of atoms, have many physical and chemical properties not observed in bulk systems. For example, bulk gold has been regarded as a poor catalyst. However, recent experimental studies¹ have shown that gold clusters in the size region of 2–6 nm, deposited on metal oxides, become active for CO oxidation at temperatures below 273 K. Examples such as this illustrate why the study of the properties of nanoparticles has become a very active field of research.

While the study of one-component metal clusters has been a subject of numerous experimental and theoretical investigations during the last two decades,^{2,3} much less attention has been devoted to the study of bimetallic clusters. A possible reason for this is the added complexity of these systems.⁴ The properties of bimetallic particles are defined not only by interatomic interactions, but also by differences in atomic sizes and relative concentrations.

Bimetallic particles have some features that considerably influence their structure and properties and which distinguish them from one-component systems. First of all is the phenomenon of surface segregation. In the case of the aluminum–nickel system considered in the present investigation, aluminum has a much lower surface free energy than does nickel [σ_s (Al) = 1140 mJ/m² vs σ_s (Ni) = 2100 mJ/m²].⁵ Therefore, aluminum atoms tend to migrate to the surface of a cluster to reduce the total free energy. Since the proportion of surface atoms in nanoparticles is very high, surface segregation may play a key role in the determination of their structure. Another phenomenon that influences structures of bimetallic particles is ordering. The enthalpy of mixing for the nickel–aluminum system is negative over a wide range of compositions.⁶ That is, since the mixing of Al and Ni is an exothermic process, a cluster would be expected to maximize the number of Ni–Al bonds. Consequently, the final structure of Ni–Al nanoparticles is the result of a competition between surface segregation and compositional ordering, and may be mediated by nonequilibrium aspects imposed by the kinetics of solidification.

In the present paper we report the results of molecular dynamics simulations of melting and freezing of Ni–Al

nanoparticles at three different compositions: Al₃Ni, a system rich in Al, NiAl of equiatomic composition, and Ni₃Al, which is rich in Ni. In the next section we present the details of computer simulations. Section 3 gives the results of computer simulations, which are discussed in Section 4. Conclusions of our study are presented in Section 5.

II. Molecular Dynamics Simulations

We have used the *N*-body potential function of Voter and Chen⁷ to simulate the properties of Ni–Al nanoparticles. This is a version of an embedded-atom model (EAM) that was parametrized to reproduce the properties of pure Ni and Al metals and their alloys. The simulations were performed with the aid of the code XMD⁸ developed at the University of Connecticut. In the present work, simulations were carried out at constant temperature. The “temperature clamp” was used to keep a system at constant temperature. This is an algorithm which scales the instantaneous velocities in order to bring the temperature to its desired value, not abruptly, but after 33 (default value) steps. Equations of motion were integrated by a fifth-order Gear predictor–corrector algorithm with a time step $\Delta t = 2.0$ fs.

As mentioned earlier, molecular dynamics simulations were performed on nanoclusters at three different compositions, Al₃Ni, NiAl, and Ni₃Al. In the bulk state these compositions form ordered alloys with different crystal structures: Al₃Ni has an ordered orthorhombic (D0₂₀) prototype structure; NiAl has an ordered cubic (B2) crystal structure isotypic with CsCl; and Ni₃Al has an ordered cubic (L1₂) structure isotypic with Cu₃Au.

The initial configurations were constructed by trimming down a cube with a bulklike crystal structure to obtain approximately spherical clusters of the desired size. That is why the ratio of aluminum and nickel atoms in particles does not necessarily correspond exactly to the initial alloy composition. Clusters were heated from 300 K with temperature steps of 100 K and equilibrated at each temperature for 40 ps. In the vicinity of the melting transition temperature, steps were reduced to 20 K. Clusters were heated 200 K above their melting points to ensure complete melting, and then cooled at a rate of 2.5×10^{12} K/s in order to observe what would happen.

We used a Common Neighbor Analysis (CNA)⁹ to identify the structure of nanoparticles. This method provides a simple

* Corresponding author.

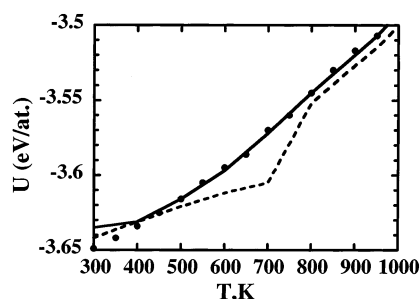


Figure 1. Temperature dependence of the configurational energy U for Al_3Ni particles with 1022 atoms. The solid line corresponds to the heating of a cluster initially possessing a bulk orthorhombic structure, a cluster which quickly became amorphous. The dashed line represents the configuration energy during the heating of a cluster with an fcc initial structure. Solid dots correspond to the cooling of a liquid cluster.

way to characterize the local environment around each atom in the cluster. We define “bond” in terms of a unit vector \mathbf{R}_{ij} connecting an atom i with its neighboring atom j that is within a given radius R_{cut} of i . We chose R_{cut} to be 3.175 Å, a distance corresponding to the position of the first minimum in the Ni–Ni pair correlation function. For each of a pair of neighbor atoms i – j , the CNA assigns a signature consisting of three indices: (1) the number of neighbors common to both atoms; (2) the number of bonds between these common neighbors; and (3) the number of bonds in the longest contiguously bonded subset. A table with CNA signatures for bulk as well as for surface atoms with different crystal structures is given in ref 10. If the local environment of a chosen atom corresponds to any of these signatures, we define that atom as “solid” to distinguish it from “liquid” atoms in the process of a cluster’s melting and solidification.

In the following sections, to avoid tedious circumlocutions, when we refer to structures as body-centered (bcc) or face-centered (fcc), we do so ignoring the distinction between Al and Ni atoms. Therefore our notation (sometimes tempered with the prefix pseudo) will deviate from that of rigorous crystallography but not from that of common usage.

III. Results

(a) Al_3Ni . At this composition, an approximately spherical cluster with 768 Al atoms and 254 Ni atoms possessing the bulk orthorhombic structure immediately lost its crystalline structure at 300 K and transformed into an amorphous aggregate. In another run, the starting cluster had been constructed to have an ordered pseudo-face-centered cubic (fcc) structure. That structure turned out to be more stable so that the cluster retained its crystalline structure until it melted over the temperature range from 700 to 800 K as is seen in the caloric curve of Figure 1. When cooled, the liquid cluster solidified again to an amorphous structure. The caloric curve during the cooling run retraced the one observed during the heating of the amorphous cluster, except for small deviations at low temperature.

Figure 2 presents a snapshot of a frozen cluster cut through its center. It is apparent that the surface layer is composed entirely of Al atoms, which are displayed by dark spheres. As discussed below, we believe that, in the case of Al_3Ni clusters, surface segregation inhibited nucleation to an ordered structure.

(b) NiAl. In computer simulations of equiatomic NiAl nanoparticles with a bulk pseudo-body-centered cubic structure, it was found that, upon heating, this structure remained stable for clusters as well as for the bulk. A cluster with 531 atoms (280 Al atoms and 251 Ni atoms) melted at approximately 1050 K, and a cluster with 1411 atoms (672 Al atoms and 739 Ni

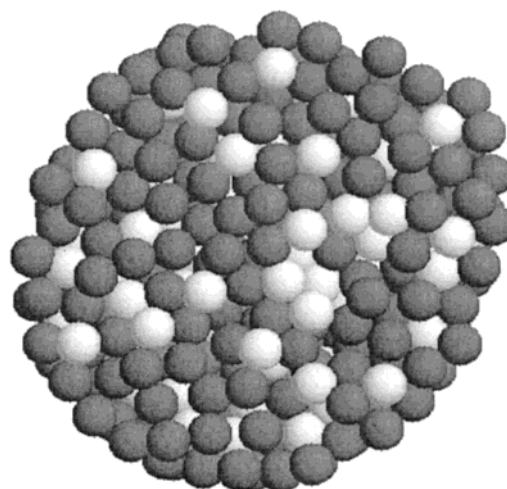


Figure 2. Snapshot of a frozen Al_3Ni nanocluster cut through its center. Dark spheres represent Al atoms and light spheres represent Ni atoms.

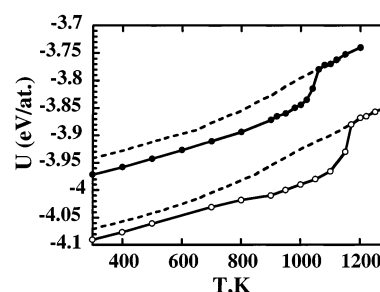


Figure 3. Temperature dependence of the configurational energy U for NiAl particles. The solid line with solid circles corresponds to the heating of a cluster with 531 atoms, and the solid line with open circles represents the heating of a particle with 1411 atoms. Dashed lines show the configurational energies during the cooling of the corresponding particles.

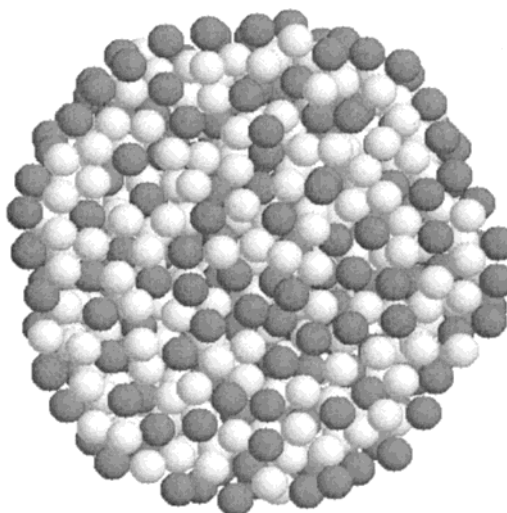


Figure 4. Same as Figure 2 except for the NiAl composition.

atoms) melted at around 1180 K. During cooling runs, the clusters solidified to an amorphous structure even though the potential energy of such disordered clusters is significantly higher than the energy of the initial ordered clusters with a cubic structure, as shown in Figure 3. A snapshot of a frozen cluster, displayed in Figure 4, again exhibits a surface segregation in NiAl nanoparticles where the surface layer consists almost entirely of Al atoms.

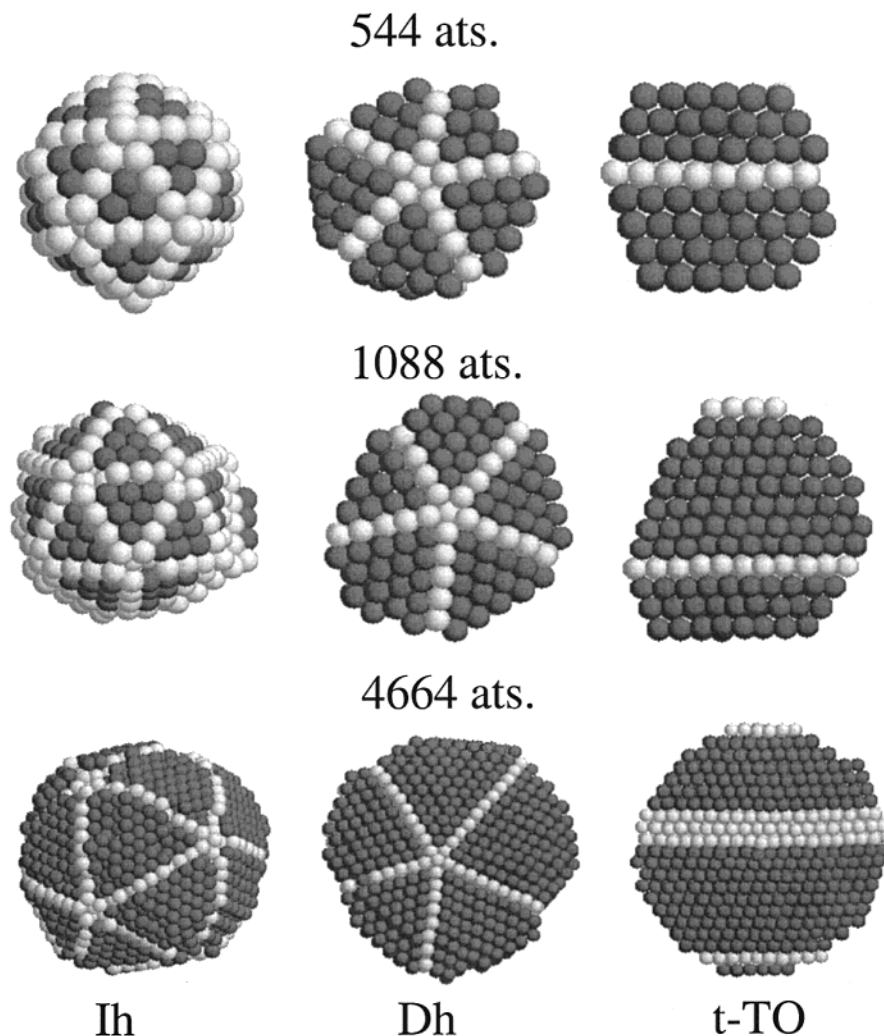


Figure 5. Typical structures spontaneously formed during the freezing of supercooled Ni_3Al nanoclusters. Dark spheres represent atoms with an fcc local structure and light spheres are atoms with an hcp environment. In this figure no distinction is made between Al and Ni atoms.

(c) Ni_3Al . In the case of this Ni-rich composition the behavior of nanoparticles during the cooling runs turns out to be completely different from that of the previous two compositions. With aluminum constituting only one-quarter of the atoms, there are not enough atoms of this low-energy component to cover the surface. This gave liquid clusters an opportunity to nucleate and freeze during the cooling runs.

Computer simulations were performed on particles of three different sizes, namely 544, 1088, and 4664 atoms. Because nucleation is a stochastic process, we thought it worthwhile to generate twenty liquid configurations for each particle size to study their freezing. Individual clusters for each size were generated and frozen under identical conditions, but they froze to various distinctly different final structures. Typical structures obtained during the freezing of Ni_3Al nanoparticles are illustrated in Figure 5. In these images, atoms of different shades have different local environments but they do not represent different identities of atoms, Al or Ni. An icosahedron (Ih) is composed of 20 distorted tetrahedra joined at the particle center with different orientations of units. Within the tetrahedral unit all atoms have the same pseudo-fcc local order. Alternatively, atoms that are located in the boundary of two tetrahedral units have a pseudohexagonal close-packed (hcp) local environment. The same is true also for decahedral (Dh) particles, which are composed of five slightly distorted truncated tetrahedra that share a common edge. In the twinned truncated octahedral (t-

TO) particles, atoms with an hcp environment are located on stacking faults of the fcc planes.

Frozen particles have a well-defined local translational order but are disordered compositionally. In Figure 6 we distinguish between the different kinds of atoms. The particle shown in Figure 6a is in its initial, ordered, fcc structure with 1088 atoms at 300 K. One of the frozen clusters with the decahedral structure is shown in Figure 6b without distinguishing between Al and Ni atoms in order to see its structure, and the same cluster is shown with the kinds of atoms identified. Clearly, the frozen particle is compositionally disordered. The same is true for the frozen particle with a twinned fcc structure, as shown in Figure 6c.

IV. Discussion

In our previous computer experiments we have observed nucleation in the crystallization of molecular,¹¹ ionic,¹² and metallic¹³ clusters. These simulations showed that the nucleation of crystalline aggregates in clusters invariably began at or very near the surface. In the present study, for those clusters in which surface segregation led to nearly pure aluminum surfaces, the low energy coating that formed seems to have inhibited surface nucleation. Such clusters solidified into amorphous masses.

On the other hand, in the example for which there was insufficient aluminum to coat the surface, entirely different

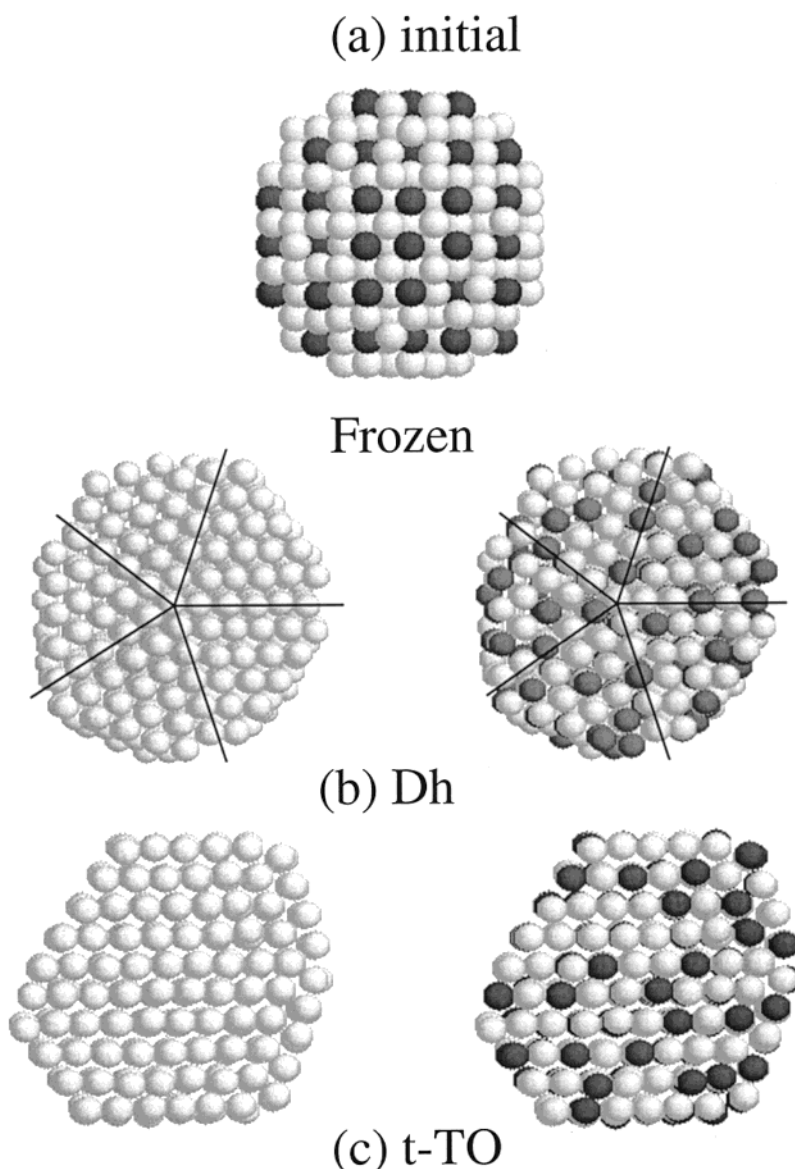


Figure 6. Images of initial and frozen Ni_3Al particles with 1088 atoms with distinctions made between the Al and Ni atoms. Dark spheres represent Al atoms, and light spheres are Ni atoms. (a) an initial ordered cluster with a pseudo-bcc cubic (B2) structure; (b) frozen cluster with a decahedral structure without the distinction (to facilitate visual recognition) and with the distinction between the different types of atoms; (c) the same as for (b) but for a frozen cluster with a twinned TO structure.

structures materialized when the clusters froze. Structures obtained upon the solidification of Ni_3Al particles are typical low-energy structures characteristic also of those for one-component metal clusters with an fcc bulk structure, such as Au,¹³ Ni,¹⁴ and Ag.¹⁵ These structures included icosahedral, decahedral, and truncated octahedral forms. Each face of an icosahedron is a (111) face, a face with the lowest surface free energy tending to make the icosahedral structure stable, especially for small cluster sizes where the surface-to-volume ratio is large. As the size of particles increases, the growing internal strain in the icosahedron^{14,16} causes an increase in the bulk contribution to the total free energy that ultimately overcomes the effect of the lowest surface energy. Note that the difference in size of Al and Ni atoms can, in principle, help to relieve the strain suffered in large icosahedral units, a factor helping to stabilize the icosahedral organization in bimetallic alloys when they freeze to “quasicrystals”.¹⁷ The truncated decahedron has some (100) faces possessing a higher surface free energy than Ih, but due to the lower internal strain¹⁴ and

the more favorable volume contribution to the total free energy, it becomes a more probable outcome at large particle sizes. On the other hand, the crystalline truncated octahedral clusters with an fcc structure have no internal strain but, instead, have a large surface energy. At larger cluster sizes, where the surface contribution becomes relatively less important, TO structures (or their twinned t-TO variant) are also obtained. The above discussion provides a rationale to account for the stabilities of different structures observed in metallic particles.

Consider now the energy of bimetallic Ni_3Al particles during the melting and heating and compare it with that for a one-component system, for example, gold particles from our previous simulations.¹³ For particle sizes in the vicinity of five hundred atoms, very nearly half the atoms are located in the surface layer. Frozen particles tend to adopt their optimal geometry or shape when their surface energy is lower than the surface energy of an initial quasi-spherical cluster. That is why frozen gold particles have a *lower* potential energy than the initial quasi-spherical one. In the case of bimetallic particles, the total energy

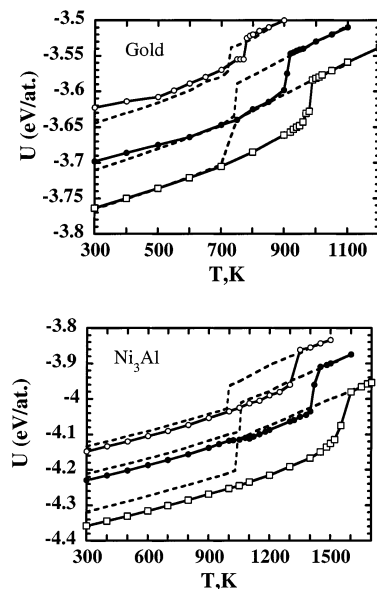


Figure 7. Comparison of the temperature dependence of the configurational energy U for gold and for Ni_3Al particles during melting and cooling. Open circles are for a gold particle with 459 atoms and an Ni_3Al particle with 544 atoms; solid circles for a gold particle with 1157 atoms and an Ni_3Al particle with 1088 atoms; squares are for a gold cluster with 3943 atoms and an Ni_3Al cluster with 4664 atoms. Solid lines correspond to heating of initial quasispherical particles with bulk fcc structures, and dashed lines represent configuration energy during the cooling of corresponding liquid clusters. The sharp drops in the dashed lines on cooling are the signatures of nucleation, a stochastic process not occurring at any specified time or temperature.

has an additional term related to compositional order. This term is responsible for the *higher* potential energy of frozen, compositionally disordered Ni–Al particles than the energy of the initial ordered spherical cluster. This is true despite the fact that frozen particles have a lower surface energy. As the size of particles increases, the surface term becomes relatively less important. Therefore, for a gold cluster with around 4000 atoms, initial spherical and frozen optimal geometries have nearly the same potential energy. On the other hand, for bimetallic Ni–Al nanoparticles the difference between the initial ordered and the frozen disordered structures increases with increasing size. These similarities and contrasts between bimetallic and one-component clusters are illustrated in Figure 7.

Why then did Ni_3Al particles freeze to a metastable compositionally disordered structure? This is due to the kinetics of solidification. In Figure 8 is portrayed a typical time evolution of the potential energy of a Ni_3Al particle with 4664 atoms during the crystallization at 1050 K. Up to 200 ps the cluster remained in its supercooled liquid state. A drop in the potential energy that started around 200 ps corresponds to the beginning of solidification. Freezing was such a very fast process, taking only approximately 150 ps to complete, that there was not enough time for atoms to order compositionally. They might

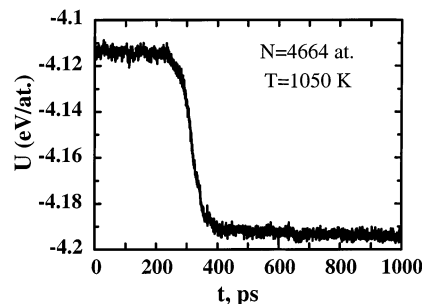


Figure 8. The time evolution of the potential energy U per atom for an Ni_3Al particle with 4664 atoms during solidification at 1050 K.

eventually have transformed into an ordered phase during a long annealing, however.

V. Concluding Remarks

Molecular dynamics simulations of bimetallic Ni–Al nanoparticles show that the composition can have a major influence on the structure to which the molten particles solidify. In the case of compositions for which there is enough aluminum to cover the surface, surface segregation of this softer metal leads to a surface coating that inhibits nucleation. This causes clusters to solidify to an amorphous structure. On the other hand, molten Ni-rich particles can nucleate and freeze in the same way as one-component particles, to various structures including icosahedral, decahedral, and other multiply twinned structures with well-defined local translational order but with compositional disorder. Presumably, the kinetics of crystallization is too fast to allow ordering during freezing.

Acknowledgment. This research was supported by a grant from the National Science Foundation.

References and Notes

- (1) Huruta, M. *Catal. Today* **1997**, 36, 153.
- (2) *Metal Clusters*; Ekardt, W., Ed.; Wiley: New York, 1999.
- (3) *Large Clusters of Atoms and Molecules*; Martin, T. P., Ed.; Kluwer: Dordrecht, 1996.
- (4) Jellinek J.; Krissinel, E. B. In *Theory of Atomic and Molecular Clusters*; Jellinek, J., Ed.; Springer: Berlin, 1999; p 277.
- (5) Miedema, A. R. *Z. Metallkde* **1978**, 69, 287.
- (6) *Selected Values of Thermodynamic Properties of Binary Alloys*; Hultgren, R., Desai, P. D., Hawkins, D. T., Gleiser, M., Kelley, K., Eds; American Society for Metals: Metals Park, OH, 1973.
- (7) Voter, A. F.; Chen, S. P. *Mater. Res. Soc. Symp. Proc.* **1987**, 82, 175.
- (8) See: //www.ims.uconn.edu/centers/simul/#Software.
- (9) Faken, D.; Jonsson, H. *Comput. Mater. Sci.* **1994**, 2, 279.
- (10) Cleveland, C. L.; Luedtke, W. D.; Landman, U. *Phys. Rev. B* **1999**, 60, 5065.
- (11) Chushak, Y. G.; Bartell, L. S. *J. Phys. Chem. B* **1999**, 103, 11196.
- (12) Huang, J.; Bartell, L. S. *J. Phys. Chem. A* **2002**, 106, 2404.
- (13) Chushak, Y. G.; Bartell, L. S. *J. Phys. Chem. B* **2001**, 105, 11605.
- (14) Cleveland, C. L.; Landman, U. *J. Chem. Phys.* **1991**, 94, 7376.
- (15) Baletto, F.; Mottet, C.; Ferrando, R. *Phys. Rev. B* **2001**, 63, 155408.
- (16) Marks, L. D. *Rep. Prog. Phys.* **1994**, 94, 603.
- (17) Shechtman, D.; Blech, I.; Gratias, D.; Cahn, J. W. *Phys. Rev. Lett.* **1984**, 53, 1951.